frontiers in Energy Research

ORIGINAL RESEARCH
published: 13 May 2021
doi: 10.3389/fenrg.2021.673758

Combining Oxidative Torrefaction and Pyrolysis of *Phragmites australis*: Improvement of the Adsorption Capacity of Biochar for Tetracycline

Shilin Jiang[1], Mengjiao Tan[1], Zhongliang Huang[1], Jinguang Hu[2], Changzhu Li[1], Tingzhou Lei[3], Xuan Zhang[1], Zijian Wu[1], Jing Huang[1], Xiaoli Qin[1] and Hui Li[1]**

[1] State Key Laboratory of Utilization of Woody Oil Resource, Hunan Academy of Forestry, Changsha China, [2] Department of Chemical and Petroleum Engineering, University of Calgary, Calgary, AB, Canada, [3] Institute of Urban and Rural Mining, Changzhou University, Changzhou, China

OPEN ACCESS

Edited by:
Wei-Hsin Chen, National Cheng Kung University, Taiwan

Reviewed by:
Kai Ling Yu, University of Malaya, Malaysia
Kit Wayne Chew, Xiamen University Malaysia, Malaysia

***Correspondence:**
Zhongliang Huang
zhongliang@hnlky.cn
Hui Li
lihuiluoyang@163.com

Specialty section:
This article was submitted to Bioenergy and Biofuels, a section of the journal Frontiers in Energy Research

Received: *28 February 2021*
Accepted: *13 April 2021*
Published: *13 May 2021*

Citation:
Jiang S, Tan M, Huang Z, Hu J, Li C, Lei T, Zhang X, Wu Z, Huang J, Qin X and Li H (2021) Combining Oxidative Torrefaction and Pyrolysis of Phragmites australis: Improvement of the Adsorption Capacity of Biochar for Tetracycline. Front. Energy Res. 9:673758. doi: 10.3389/fenrg.2021.673758

The objective of this study was to evaluate the effect of oxidative torrefaction on the biochar characteristics of *Phragmites australis* (PAS) and its tetracycline (TC) adsorption capacity. Oxidative torrefaction combined with pyrolysis of PAS was performed, and the physicochemical properties of the biochar were characterized. Subsequently, the effects of adsorbent dosage, initial TC concentration, salinity, and temperature on the TC adsorption capacity of PAS biochar were evaluated; the kinetic, equilibrium, and thermodynamic results were used to assess the adsorption mechanism. The results showed that the biochar derived from oxidatively torrefied PAS pyrolysis (TPBC) had higher specific surface area and lower ash content than the biochar derived from raw PAS pyrolysis (PBC). TPBC showed a higher TC adsorption capacity than PBC. The adsorption kinetics were more in agreement with pseudo-second-order model than pseudo-first-order and intraparticle diffusion models. The rate of adsorption by PAS biochar was controlled by external mass transfer and intraparticle diffusion, and the adsorption process was favorable and irreversible. Moreover, the dominant mode of adsorption is physical, and the organic functional groups of PAS biochar participate in the adsorption process. In summary, oxidative torrefaction could be an effective approach for improving the TC adsorption capacity of PAS biochar.

Keywords: biomass, Wetland plant, oxidative torrefaction, pyrolysis, biochar, tetracycline

HIGHLIGHTS

- TPBC was produced by combining oxidative torrefaction and pyrolysis of PAS.
- Oxidative torrefaction led higher specific surface area of PAS biochar.
- PBC showed higher tetracycline adsorption capacity than PBC.
- TC adsorption was controlled by external mass transfer and intraparticle diffusion.
- PAS biochar is promising adsorbent for treatment of wastewater containing TC.

INTRODUCTION

Multiple antibiotics used in the medicinal, livestock, and poultry breeding industries have detrimental effects on human and animal health, and have thus led to great concern in recent years. Most antibiotics are excreted into the natural environment as prototypes or metabolites, resulting in environmental pollution. The primary sources of antibiotics in the water environment include sewage treatment plant wastewater, chemical manufacturing wastewater, animal husbandry, and aquaculture. Tetracycline (TC), one of the most widely used antibiotic, is widespread and frequently detected in the water environment. TC is easy to remain in water environment for a long time and cause environmental harm, mainly manifested in its adverse effects on non-target organisms. Long-term exposure of organisms to the antibiotic environment will produce chronic toxicity, which can cause negative effects on terrestrial and aquatic ecosystems, and damage the balance of the ecosystem. Moreover, the highly soluble TC is easily transferred to other environmental media via the water environment and must be removed in a technically, environmentally, and economically acceptable manner.

Common methods for removing TC from wastewater include photocatalytic degradation (Zhu et al., 2019b), membrane separation (MABR) (Taşkan et al., 2019), adsorption (Song et al., 2019), and anaerobic digestion (Zhang et al., 2018). Among these methods, adsorption is important because it is simple, inexpensive, and highly efficient at low TC concentrations. In addition, no toxic intermediates or by-products are produced during the adsorption process (Jang and Kan, 2019). Biochar, which is created by the pyrolysis of biomass or organic waste, has attracted considerable attention for wastewater treatment owing to its high specific surface area, developed pore structure, and strong hydrophobicity (Xiang et al., 2020). However, the physicochemical properties of biochar vary widely due to various feedstocks and production conditions (Lyu et al., 2020; Su et al., 2020; Yu et al., 2017). Therefore, most biochars need to be chemically modified to achieve good TC adsorption capacity (Liu et al., 2019; Liu et al., 2021; Nguyen et al., 2021; Wang et al., 2021), which increases production costs.

Torrefaction, also called low-temperature pyrolysis, is an effective pretreatment method for upgrading biomass. In the torrefaction process, biomass is heated at modest temperatures of 200–300°C in an inert or oxidative atmosphere; the carrier gas (oxygen) content in oxidative torrefaction generally varies from 3 to 16 vol.%. Biomass combustion gas is commonly used as a carrier gas for oxidative torrefaction to control production costs (Uemura et al., 2017). After torrefaction, the torrefied biomass has more uniform properties, improved grindability and reactivity, lower moisture content, lower H/C and O/C atomic ratios, and higher energy densities or heating values (Peng et al., 2013; Tumuluru, 2015; Xu et al., 2018). Moreover, multiple studies have shown that torrefaction has varying degrees of effect

Abbreviations: TC: tetracycline; PAS: *Phragmites australis*; PBC: the biochar derived from raw PAS pyrolysis; TPBC: the biochar derived from oxidatively torrefied PAS pyrolysis.

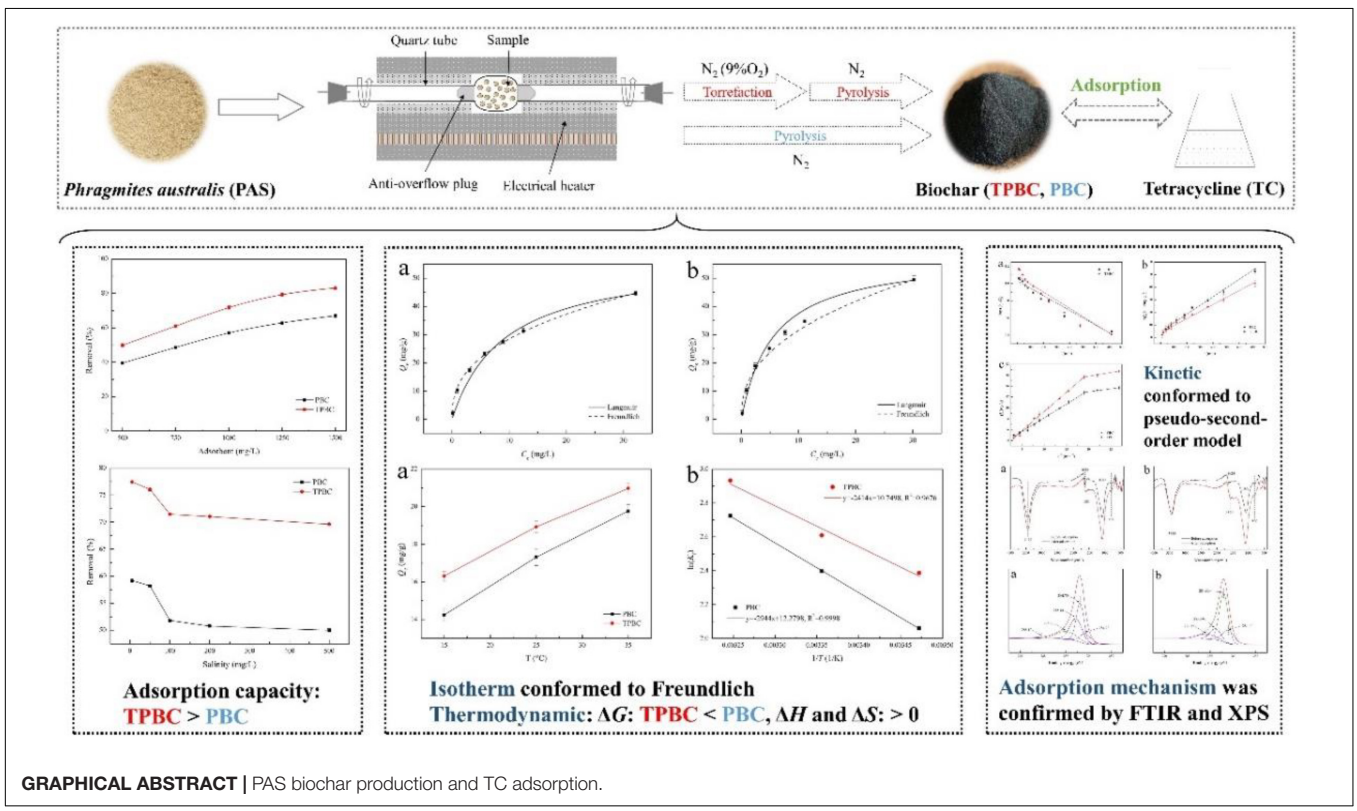

GRAPHICAL ABSTRACT | PAS biochar production and TC adsorption.

on the characteristics and kinetics of pyrolysis and the properties of the products (Meng et al., 2012; Chen et al., 2015; Bach et al., 2017; Wang et al., 2017).

Most of the research on torrefaction has been the improvement of fuel properties of biomass in recent years (Gan et al., 2018). There are few researches on combining torrefaction and pyrolysis, especially combining oxidative torrefaction and pyrolysis, which may limit the development of torrefaction technology and product application. The principal products of biomass pyrolysis are biochar, gas, and condensables (bio-oil, tar, and water), whose ratio and chemical composition are seriously affected by the torrefaction process (Wannapeera et al., 2011). In the pyrolysis process, cellulose and trace hemicelluloses are the principal sources of bio-oil, while biochar is derived from lignin (Chen et al., 2016). The pyrolysis of torrefied biomass produces less bio-oil and tar and more biochar when increasing torrefaction temperatures are used (Wannapeera et al., 2011; Ren et al., 2013; Ren et al., 2014; Doddapaneni et al., 2016). On the one hand, Gogoi et al. (2017) revealed that biochar from torrefied biomass showed improved adsorption performance compared to that of non-torrefied biomass. On the other hand, Chen et al. (2017) reported a decreased specific surface area. Zhu et al. (2019a) proposed a torrefaction pretreatment combined with co-pyrolysis to produce biochar from walnut shells and bio-oil distillation residue. Torrefaction pretreatment was beneficial for the evolution of large aromatic rings in biochar to small aromatic rings and for the formation of ordered carbon. Fleig et al. (2021) reported that torrefaction pretreatment increased the specific surface area of rice husk biochar from 1.5 m^2/g to a maximum of 16.7 m^2/g, and the sample with torrefaction and pyrolysis at 500°C presented the highest biochar yield. Lampropoulos et al. (2020) found that olive kernel biochar, with less-ordered structures, increased C and ash contents, and higher porosity, was obtained by torrefaction combined with pyrolysis. Thus, targeted torrefaction pretreatments must be performed for different biomass types and specific product applications.

Phragmites australis (PAS) is one of the most common plants in natural and artificial wetlands in China and has a high annual yield. As a traditional biomass, PAS is a good raw material for biochar production. In this study, PAS biochar was prepared by pyrolysis combined with oxidative torrefaction. Compared with the biochar derived from the pyrolysis of non-torrefied PAS and non-oxidatively torrefied PAS, biochar derived from oxidatively torrefied PAS pyrolysis had a higher specific surface area and lower ash content; these characteristics indicated that the biochar derived from oxidatively torrefied PAS may have better adsorption performance. Therefore, oxidative torrefaction may be an effective approach for improving the adsorption capacity of PAS biochar for TC. The PAS biochar may be effective adsorbent for treatment of wastewater containing TC, which may effectively remove TC and reduce the cost of biochar production.

Hence, oxidative torrefaction combined with pyrolysis of PAS was performed in this study, which aimed to evaluate the effect of oxidative torrefaction on PAS biochar characteristics and its TC adsorption capacity. The physicochemical properties of PAS biochar that were characterized included surface functional groups, crystalline structure, surface chemical composition, and specific surface area. The effects of adsorbent dosage, initial TC concentration, salinity, and temperature on the TC adsorption capacity of PAS biochar were evaluated, and the kinetic, equilibrium, and thermodynamic results were used to assess the adsorption mechanism. In addition, the TC adsorption capacity of the biochar derived from pyrolysis of oxidatively torrefied PAS and several biochars produced from different types of biomass were compared to evaluate the application potential of PAS biochar.

MATERIALS AND METHODS

Materials

The PAS was collected from the Yanghu Wetland, Hunan Province, China. Prior to the experiment, the raw material was dried at 105°C for 24 h, crushed into fractions with particle sizes of 0.15–0.25 mm, and stored in a sealed bag at 4°C. Tetracycline purchased from Shanghai Ryon Biotechnology Co., Ltd.

Torrefaction and Pyrolysis

The oxidative torrefaction experiments were performed in a rotary tube furnace. During each run, approximately 50 g of dried PAS was placed in the reactor. In the heating procedure, the temperature was increased from room temperature to 270°C at 3°C/min and the temperature was maintained for 30 min; the carrier gas (flow rate = 200 SCCM) consisted of nitrogen containing 9 vol.% of oxygen. After torrefaction, the PAS was pyrolyzed in a rotary tube furnace, and pure nitrogen was used as the carrier gas. In the heating program, the temperature was increased from room temperature to 675°C at 3°C/min and then maintained for 120 min. For comparison, the raw PAS was pyrolyzed in a rotary tube furnace under the same conditions. Notably, torrefaction and pyrolysis are continuous processes. Therefore, the effect of property changes that occur during the storage of torrefied PAS on the biochar properties was avoided. The biochars derived from raw and oxidatively torrefied PAS pyrolysis were denoted PBC and TPBC, respectively.

Characterization of Biochar

The surface functional groups of the biochar were identified using Fourier-transform infrared (FTIR, Bruker Vertex 70) spectroscopy. An X-ray diffractometer (XRD, X'Pert PRO MPD) with a Cu Kα radiation source was used to investigate the crystalline structure of the biochar. The surface chemical composition was analyzed by multifunctional X-ray photoelectron spectrometry (XPS, Thermo ESCALAB 250XI). The specific surface area and pore diameter were measured using a surface area analyzer (TriStar II 3flex).

Adsorption Experiments

Batch Adsorption

Tetracycline solution (50 mg/L) was prepared by dissolving 0.1 g tetracycline in 2 L ultrapure water. To investigate the effect of biochar dosage on the TC adsorption capacity of biochar, different amounts of adsorbent (0.025–0.075 g) were added to

250 mL conical flasks with 50 mL TC. The conical flasks were shaken in a constant-temperature shaking incubator at 150 rpm for 24 h, and the environmental temperature was controlled at 25°C, except for the thermodynamic studies. The TC concentration was determined by ultraviolet-visible spectrometry at a wavelength of 359 nm. The calibration curve was constructed by plotting the absorbance versus the concentration of standard TC solutions ranging from 0 to 50 mg/L.

To investigate the effect of TC concentration on the TC adsorption capacity of biochar, 0.0625 g of adsorbent was added to 50 mL of TC solutions with initial concentrations of 5–50 mg/L. To check the effect of salinity on TC adsorption, different amounts of NaCl were added to the samples to adjust their salinity in the range 5–500 mg/L. The adsorption kinetic experiments were conducted at a biochar dosage of 0.02 g per 50 mL and a TC concentration of 10 mg/L. The TC concentrations were then measured at different time intervals. The adsorption isotherm experiments were conducted at a biochar dosage of 0.02 g per 50 mL and TC concentrations of 1–50 mg/L. To investigate the effect of temperature on the TC adsorption capacity of biochar, 50 mL of 10 mg/L TC and 0.02 g of biochar were mixed at different temperatures (15, 25, and 35°C). All the tests were repeated three times.

The removal percentage is calculated by Eq. (1)

$$Re = \frac{c_1 - c_2}{c_1} \tag{1}$$

The adsorption capacities are calculated by Eq. (2)

$$Q = \frac{v(c_1 - c_2)}{m} \tag{2}$$

where Re, c_1, c_2, Q, v, and m represent the removal percentage (%), the solution concentration before adsorption (mg/L), the solution concentration after adsorption (mg/L), the adsorption capacity (mg/g), the solution volume (mL), the adsorbent mass (g).

Adsorption Kinetic

Using OriginPro 8.5 software, TC adsorption on biochar was studied by fitting the pseudo-first order, pseudo-second order, and intraparticle diffusion kinetics (Chabi et al., 2020).

The pseudo-first order equation is shown in Eq. (3):

$$log\,(Q_e - Q_t) = logQ_e - \frac{k_1}{2.303}t \tag{3}$$

The pseudo-second order equation is shown in Eq. (4):

$$\frac{t}{Q_t} = \frac{1}{k_2 Q_e^2} + \frac{t}{Q_e} \tag{4}$$

The intraparticle diffusion equation is shown in Eq. (5):

$$Q_t = k_{id}t^{1/2} + C \tag{5}$$

where Q_t, Q_e, t, k_1, k_2, k_{id}, α, and β represent the adsorption capacity at time t (mg/g), the equilibrium adsorption capacity (mg/g), the adsorption residence time (min), the pseudo-first-order rate constant (h^{-1}), the pseudo-second order rate constant [mg/(g h)], the intraparticle diffusion rate constant [mg/(g $h^{0.5}$)], the initial adsorption coefficient [mg (g/min)], and the desorption rate constant (g/mg).

Adsorption Isotherm

TC adsorption on biochar was studied by fitting the Langmuir and Freundlich isotherms.

The Langmuir equation is given by Eqs. (6) and (7), as follows:

$$Q_e = \frac{K_L Q_m C_e}{1 + K_L C_e} \tag{6}$$

$$R_L = \frac{1}{1 + K_L C_0} \tag{7}$$

The Freundlich equation is shown in Eq. (8):

$$Q_e = K_f C_e^{1/n} \tag{8}$$

where Q_e, K_L, Q_m, C_0, C_e, K_f, and n represent the equilibrium adsorption capacity (mg/g), the Langmuir characteristic adsorption constant (L/g), the maximum adsorption capacity (mg/g), the initial concentration of the solution (mg/L), the adsorption equilibrium concentration (mg/L), the Freundlich adsorption capacity parameter, and the Freundlich index, respectively. The R_L value indicates the type of adsorption: $R_L = 0$ indicates irreversible adsorption, $0 < R_L < 1$ denotes favorable adsorption, $R_L = 1$ indicates linear adsorption, and $R_L > 1$ denotes unfavorable adsorption.

Adsorption Thermodynamic

ΔG was calculated using the K_f value obtained from the Freundlich equation of the adsorption isotherm (Ahmad and Alrozi, 2011).

$$\Delta G = -RTlnK_f \tag{9}$$

$$\Delta G = \Delta H - T\Delta S \tag{10}$$

$$lnK_f = \Delta S/R - \Delta H/(RT) \tag{11}$$

where ΔG, ΔS, ΔH, R, and T represent the Gibbs free energy (kJ/mol), the adsorption entropy change (J/(mol K)), the adsorption enthalpy change (kJ/mol), the perfect gas constant (8.314 J/(mol K), and the thermodynamic temperature (K), respectively.

RESULTS AND DISCUSSION

Biochar Characterization

Table 1 shows that the specific surface areas of the PBC and TPBC were 307.579 and 350.855 m^2/g, respectively. The average pore diameters of PBC and TPBC were 1.954 and 1.979 nm, respectively, indicating that the pore types of the biochars were primarily micropores and mesopores. Compared with other similar studies, the biochars obtained from this study had higher

TABLE 1 | The specific surface areas of the PBC and TPBC, and comparison of the results with similar studies.

Biochar type	Specific surface area (m^2/g)	Preparation method	References
Phragmites australis (PBC)	307.579	Pyrolysis	*This study*
Phragmites australis (TPBC)	350.855	Combining oxidative torrefaction and pyrolysis	*This study*
Rice straw	2.17	Combining non-oxidative torrefaction and pyrolysis	Chen et al., 2017
Rice husk	16.7	Combining non-oxidative torrefaction and pyrolysis	Fleig et al., 2021
Olive Kernel	<3	Combining non-oxidative torrefaction and pyrolysis	Lampropoulos et al., 2020

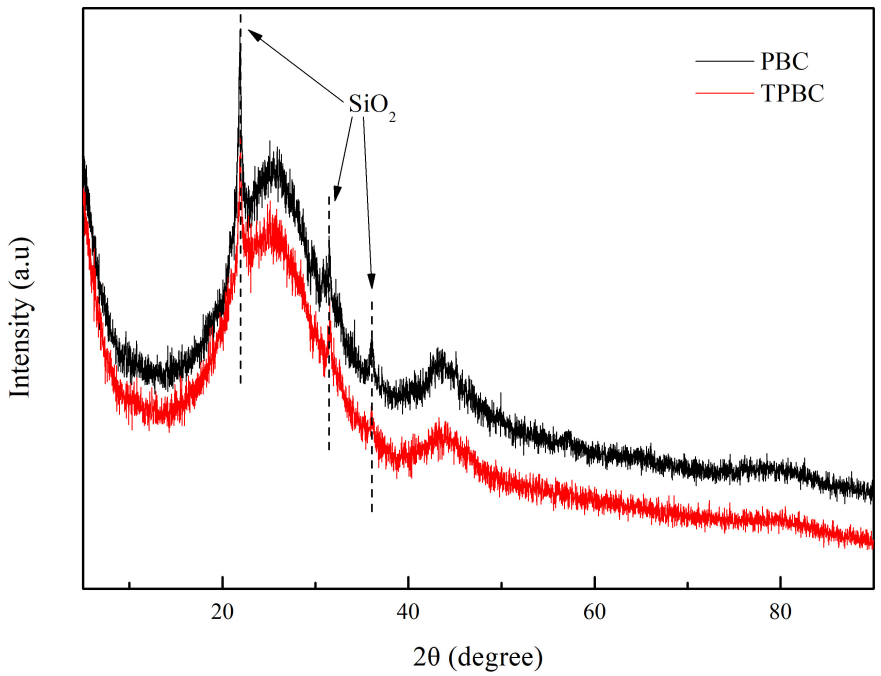

FIGURE 1 | The XRD pattern of the biochars.

specific surface areas. **Figure 1** shows that PBC and TPBC showed similar XRD diffraction peak patterns, indicating that oxidative torrefaction had no significant effect on the crystal type of the PAS biochar. The spikes appearing at 21.94°, 31.45°, and 36.08° were related to SiO_2. The TPBC peak was slightly lower than that of PBC, indicating that TPBC contained lower ash content than PBC, which may be more advantageous for TC adsorption. In summary, TPBC may have better adsorbent properties than PBC, which may facilitate TC adsorption.

Effective Parameters on TC Adsorption

Effect of Biochar Dosage

A higher adsorbent dosage generally leads to a greater removal efficiency of the adsorbate. **Figure 2** shows that the removal efficiency of TC by TPBC was significantly higher than that of PBC with different biochar dosages. When the biochar dosage was increased from 500 to 1500 mg/L, the removal efficiency of TC by PBC increased from 39.52 to 67.01%, and the removal efficiency of TC by TPBC increased from 49.93 to 83.13%, perhaps due to the growth of adsorption sites (Chabi et al., 2020). Moreover, the growth rate of the TC removal efficiency increased when the biochar dosage was increased from 500 to 1,250 mg/L, whereas the growth rate of the TC removal efficiency decreased when the biochar dosage was 1,500 mg/L. Therefore, the appropriate biochar dosage was 1,250 mg/L.

Effect of TC Concentration

Figure 3 shows that the adsorption capacity and removal efficiency of TC by TPBC were significantly higher than those of PBC with different initial TC concentrations. By increasing the TC concentration from 5 mg/L to 50 mg/L, the removal efficiency of TC by PBC decreased from 99.34 to 67.01%, and the removal efficiency of TC by TPBC decreased from 99.79 to 83.13%. The higher removal efficiency at lower initial concentrations is due to the sufficient number of adsorption sites for TC adsorption (Chabi et al., 2020). However, the ratio of adsorption sites to TC molecules decreased with increasing TC concentration, decreasing the sites available for TC adsorption. The maximum adsorption capacities of TC by PBC and TPBC were 23.69 and 27.71 mg/g, respectively. Generally, a higher TC concentration provides a stronger driving force for the adsorption reaction. Therefore, the adsorption capacity increases with increasing TC

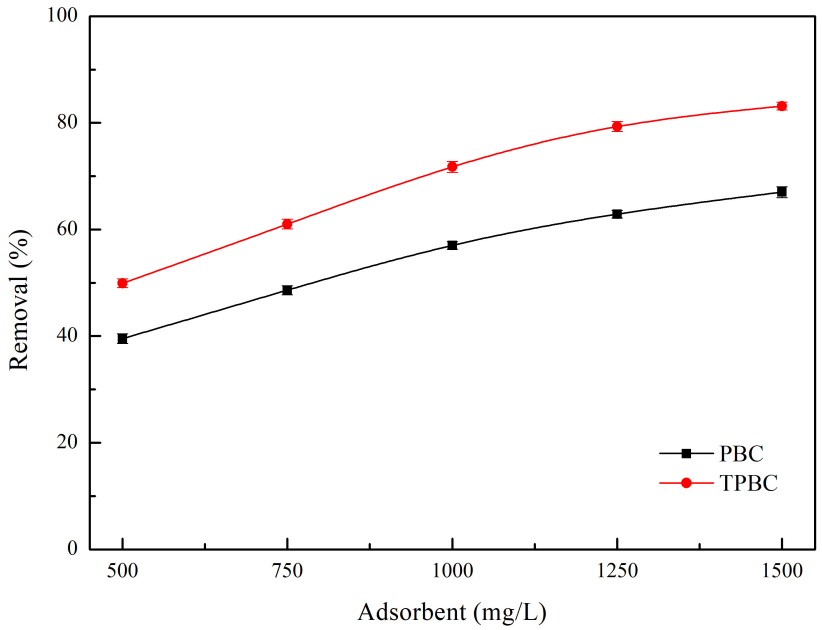

FIGURE 2 | The effect of the biochar dosage on the TC removal.

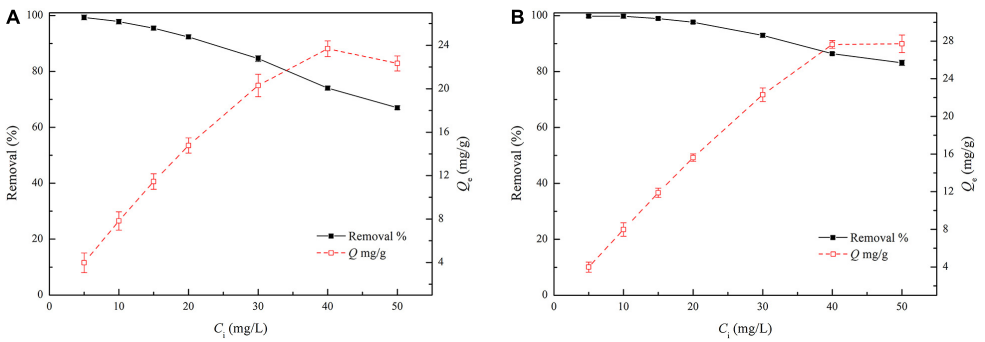

FIGURE 3 | The effect of the initial TC concentration on the adsorption capacity and removal percentage. **(A)** PBC and **(B)** TPBC.

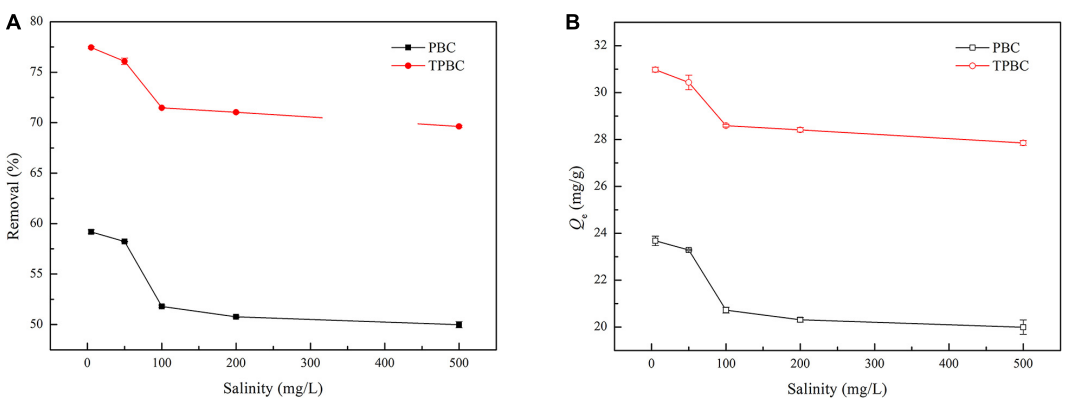

FIGURE 4 | The effect of the salinity on the removal percentage **(A)** and adsorption capacity **(B)**.

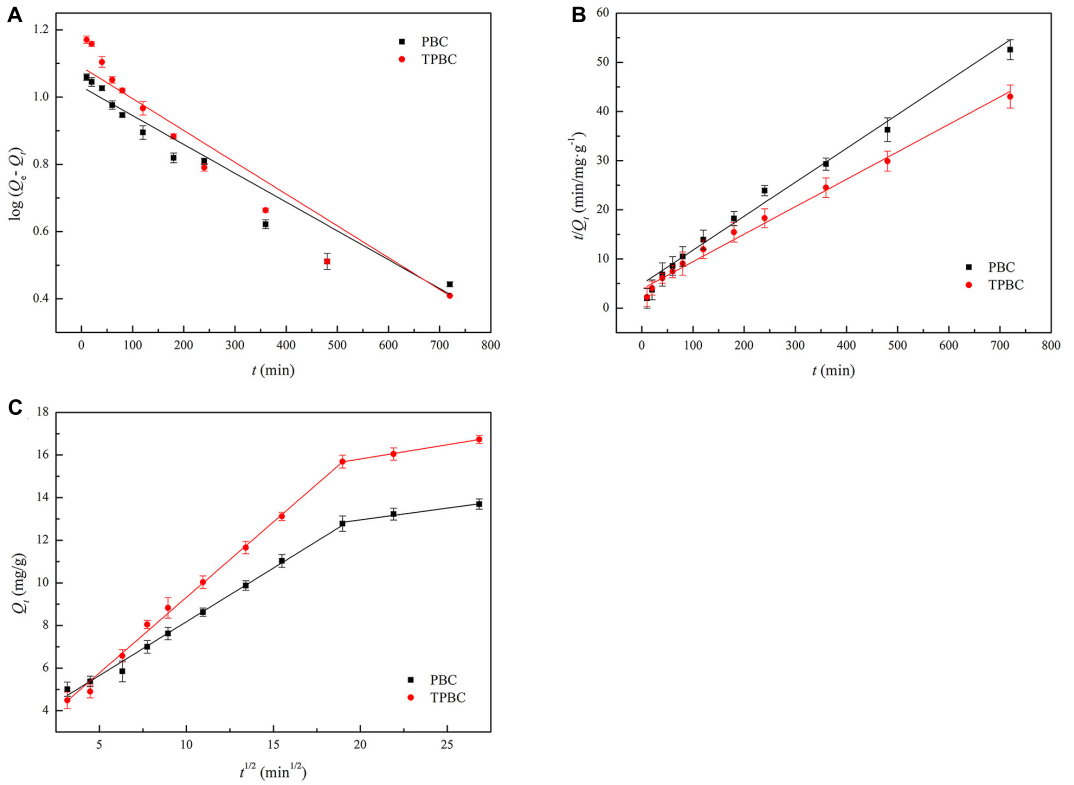

FIGURE 5 | Kinetic modeling of TC adsorption on the surface of the biochars using the pseudo-first-order **(A)** pseudo-second-order **(B)**, and intraparticle diffusion **(C)** models.

concentration, which agrees with Le Chatelier's principle (Leng et al., 2015; Gupta et al., 2020).

Effect of Salinity

Figure 4 shows that salinity had a significant effect on the removal percentage and adsorption capacity. By increasing the salinity from 5 to 500 mg/L, the removal efficiency of TC by PBC decreased by 59.18–49.98%, and the removal efficiency of TC by TPBC decreased from 77.44 to 69.64%. The adsorption capacities of TC by PBC and TPBC decreased by 23.67–19.99 mg/g by 30.98–27.85 mg/g, respectively. The decrease in removal percentage and adsorption capacity could be due to the ions competing with TC for adsorption on the ionic sites of the biochar through electrostatic interactions (Gao et al., 2012). Moreover, the removal percentage and adsorption capacity of TPBC decreases less than those of PBC, indicating a stronger anti-interference ability.

Kinetic Studies

The kinetic study was performed using pseudo-first-order, pseudo-second-order, and intraparticle diffusion models. The corresponding linear plots and kinetic parameters are presented in **Figure 5** and **Tables 2**, **3**, respectively. **Table 2** shows that the equilibrium adsorption capacities of PBC calculated by the pseudo-first order and pseudo-second order models were 10.7340 and 14.4886 mg/g, respectively; the equilibrium adsorption capacities of TPBC calculated by the pseudo-first-order and pseudo-second-order models were 12.3010 and 17.9019 mg/g, respectively. The higher equilibrium adsorption capacities for TPBC are consistent with the related experimental data. Moreover, the R^2-values of the pseudo-second-order model (0.9663 for PBC and 0.9157 for TPBC) were higher than those of the pseudo-first-order model (0.9773 for PBC and 0.9901 for TPBC), indicating that the adsorption kinetics of TC by

TABLE 2 | Kinetic parameters of pseudo-first-order and pseudo-second-order for the TC adsorption.

Samples	Pseudo-first-order			Pseudo-second-order		
	Q_e	k_1	R^2	Q_e	k_2	R^2
PBC	10.7340	0.0020	0.9663	14.4886	0.0010	0.9773
TPBC	12.3010	0.0022	0.9157	17.9019	0.0008	0.9901

TABLE 3 | Kinetic parameters of intraparticle diffusion for the TC adsorption.

Samples	Intraparticle diffusion (First linear part)			Intraparticle diffusion (Second linear part)		
	k_{id}	C	R^2	k_{id}	C	R^2
PBC	0.5048	3.1247	0.9963	0.1105	10.7477	0.9678
TPBC	0.7087	2.2299	0.9948	0.1337	13.1409	0.9987

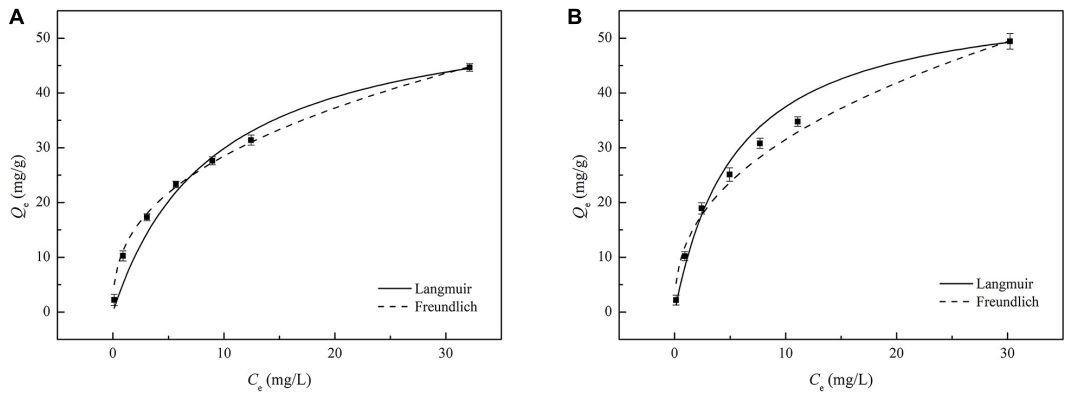

FIGURE 6 | The adsorption isotherm data of TC adsorption on PBC **(A)** and TPBC **(B)** investigated using a non-linear method.

TABLE 4 | The calculated parameters of different adsorption isotherms using linear regression at 25°C.

Samples	Langmuir				Freundlich		
	Q_m	K_L	R_L	R^2	K_f	n	R^2
PBC	57.1297	0.1096	0.1543–0.9012	0.9900	11.6650	2.5804	0.9965
TPBC	58.3554	0.1796	0.1002–0.8477	0.9926	12.2860	2.4455	0.9954

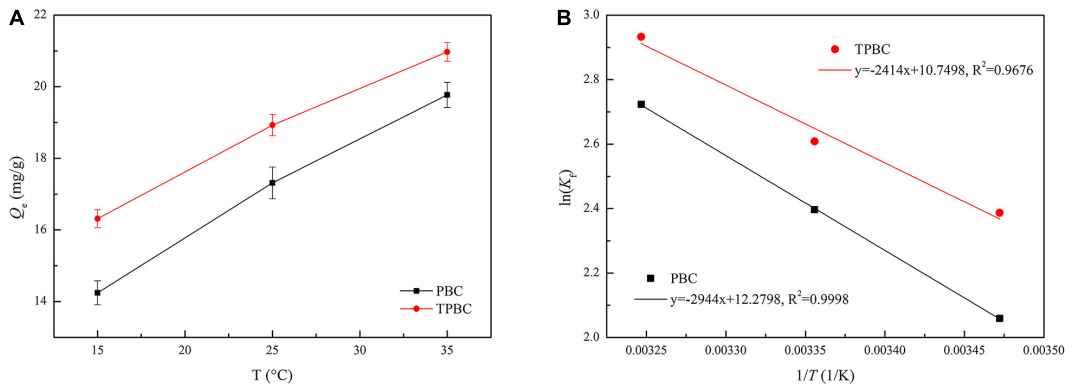

FIGURE 7 | Temperature effect on the TC adsorption by the biochars **(A)** and the Van't Hoff plot for adsorption of TC on the biochars **(B)**.

PAS biochar were in better agreement with the pseudo-second-order model.

The intraparticle diffusion model is used to describe the diffusion and mass transfer processes of the adsorbate inside and outside the adsorbent (Módenes et al., 2021). According to **Figure 5C** and **Table 3**, two-stage fitting was used for the intraparticle diffusion model; the linear plot contained two parts with different slopes. The first linear segment of the curve belongs to the rapid adsorption stage, in which TC is transported to the surface of PAS biochar, while the other linear segment is considered to diffuse through small pores (Adebayo et al., 2014). The linear part of the first linear plot cannot pass through the origin, indicating that intraparticle diffusion is not the only controlling mechanism (Adesemuyi et al., 2020). The concentration gradient decreased as the contact time increased and the TC concentration decreased, resulting in a low external mass transfer. Therefore, the adsorption rate was controlled by external mass transfer and intraparticle diffusion. Furthermore, the intercept of the second part is not zero, confirming that the adsorption reaction is also controlled by other steps (Chabi et al., 2020).

TABLE 5 | Thermodynamic parameters of TC adsorption on biochars.

Samples	T (K)	lnK_f	ΔG (kJ/mol)	ΔH (kJ/mol)	ΔS (kJ/mol)
PBC	288	2.0594	−4.9312	24.4765	0.1021
	298	2.3966	−5.9377		
	308	2.7233	−6.9737		
TPBC	288	2.3870	−5.7156	20.0708	0.0888
	298	2.6085	−6.4627		
	308	2.9327	−7.5098		

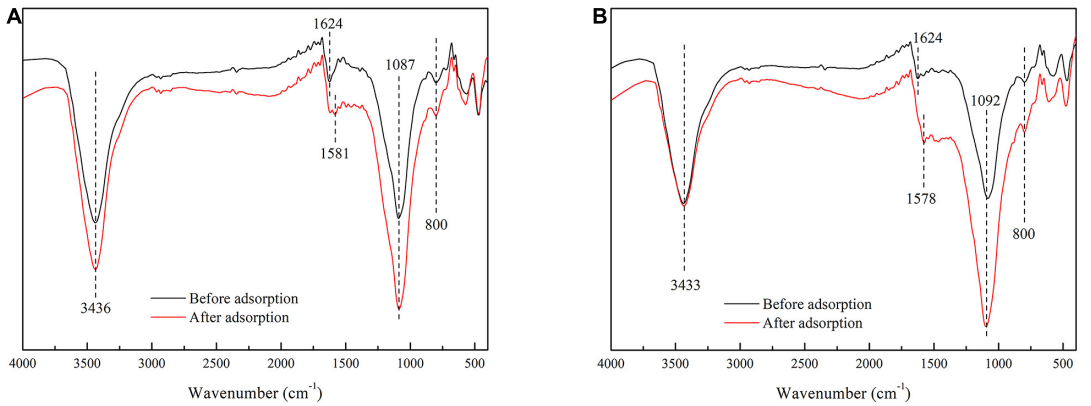

FIGURE 8 | The FTIR spectra of PBC **(A)**, and TPBC **(B)** before and after adsorption.

Isotherm Studies

The equilibrium study can explain the relationship between the concentration of adsorbate in the solution and the amount of adsorption on the surface of the adsorbent during solid-liquid equilibrium (dos Reis et al., 2016). In this study, TC adsorption was investigated using the Langmuir and Freundlich isotherms. The constants and parameters were estimated for the two models using non-linear regression. The corresponding linear plots and calculated parameters are presented in **Figure 6** and **Table 4**, respectively. **Table 4** shows that the maximum adsorption capacity of TPBC calculated by the Langmuir model was slightly higher than that of PBC, indicating that PBC and TPBC had similar maximum adsorption capacities. However, according to the actual experimental data, the adsorption capacity of TC by PBC was significantly lower than that of TPBC at the same adsorption residence time, indicating that TPBC had a higher adsorption rate than PBC. Therefore, oxidative torrefaction promoted the TC adsorption of PAS biochar.

Larger Langmuir constant values typically correspond to greater affinity of the adsorbate toward the adsorbent. The K_L of PBC (0.1096) was lower than that of TPBC (0.1796), indicating the greater affinity of TPBC toward TC. Similarly, the K_f of PBC (11.6650) was lower than that of TPBC (12.2860), indicating the higher TC adsorption capacity of TPBC. The R_L values of PBC and TPBC calculated by the Langmuir isotherm were 0.1543–0.9012 and 0.1002–0.8477, respectively, indicating a favorable adsorption process. Simultaneously, the n values of PBC and TPBC calculated by the Freundlich isotherm were 2.5804 and 2.4455 ($1/n \approx 0.39$ and 0.41), respectively, indicating favorable adsorption. The Freundlich model assumes that the surface-active sites are not equivalent, showing a heterogeneous surface. In addition, the adsorption strength decreases with increasing number of occupied sites (Areco et al., 2012; Baghdadi et al., 2016).

Thermodynamic Studies

The thermodynamic studies can explain the spontaneity, feasibility and other thermodynamic information of the adsorption process (Su et al., 2021). The effect of temperature on TC adsorption on the biochar is depicted in **Figure 7**. The adsorption capacity increased with increasing temperature, indicating that TC adsorption by the biochars is an endothermic process. In addition, the TC adsorption capacity of TPBC was higher than that of PBC at different temperatures.

Table 5 shows that the ΔH values of PBC and TPBC were 24.4765 and 20.0708 kJ/mol, respectively, confirming that the adsorption process is endothermic. Simultaneously, the ΔH values of PBC and TPBC were < 40 kJ/mol, indicating that the dominant adsorption mode was physical. Therefore, TC adsorption by PAS biochar was primarily physical. The ΔS values of PBC and TPBC were positive (0.1021 and 0.0888 kJ/mol, respectively), indicating that the adsorption process is irreversible. The Gibbs free energy (ΔG) values of PBC were calculated as −4.9312, −5.9377, and −6.9737 kJ/mol at 288, 298, and 308 K, respectively. The ΔG values of TPBC were calculated as −5.7156, −6.4627, and −7.5098 kJ/mol at 288, 298, and 308 K, respectively. The ΔG values of PBC and TPBC were negative, indicating that adsorption was a spontaneous process (Baghdadi et al., 2016). ΔG values decreased as the temperature increased, indicating enhanced adsorption at high temperatures. Moreover, the ΔG values of PBC were higher than those of TPBC at different temperatures, indicating that TPBC adsorbed TC more easily than did PBC.

Adsorption Mechanism

The higher TC adsorption capacity of TPBC than of PBC was the result of torrefaction pretreatment. In the oxidative process, devolatilization and thermal decomposition of PAS and oxidation reactions occur, resulting in better physicochemical properties of oxidatively torrefied PAS (Huang et al., 2020). Therefore, after the subsequent pyrolysis process, the obtained TPBC had a higher specific surface area, stronger hydrophobicity, and lower ash content, which led to a higher TC adsorption capacity. Kinetic, isotherm, and thermodynamic data reveal that the TC adsorption rate by PAS biochar was controlled by external mass transfer and by intraparticle diffusion; the adsorption process is favorable and irreversible, and the dominant adsorption mode is physical. For a more detailed analysis of the adsorption mechanism, the

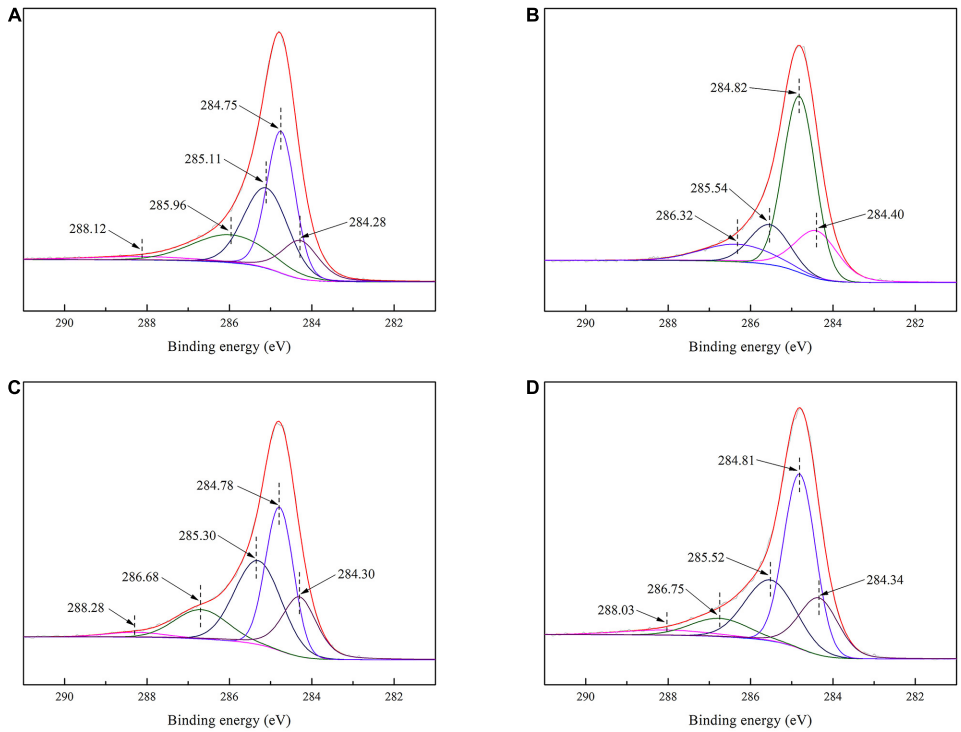

FIGURE 9 | The C1s XPS spectrum of PBC before **(A)** and after **(C)** adsorption and TPBC before **(B)** and after **(D)** adsorption.

TABLE 6 | Data of TC removal using biochars reported in various studies.

Biochar type	Pyrolysis temperature (°C)	Q_m (mg/g)	Equilibrium model that predicted the Q_m	References
Sugarcane bagasse	300	11.56	Langmuir	Divband Hafshejani et al., 2016
Bamboo biochar/montmorillonite composite	460	8.516	Langmuir	Viglašová et al., 2018
Populus alba poplar wood	500	15.92	Langmuir	Zhang et al., 2021
Oak sawdust	600	8.940	Langmuir	Wang et al., 2015
Grapefruit peel	600	47.06	Langmuir	Yu et al., 2020
Birch wood	700	3.970	Langmuir	Sanford et al., 2019
Phragmites australis	675	58.3554	Langmuir	*This study*

FTIR and XPS data before and after adsorption were used to investigate the role of organic functional groups in the biochars during adsorption.

Figure 8 shows that PBC and TPBC had similar FTIR spectra. The observed peaks at 3,436 and 3,433 cm^{-1} primarily correspond to the O-H stretching of water (Khan et al., 2020; Ntzoufra et al., 2021). The peak at 1624 cm^{-1} is attributed to the stretching vibrations of C = O and aromatic C = C (Xu et al., 2020). The peaks at 1,581 and 1,578 cm^{-1} were attributed to the stretching vibration of skeletal C = C (Zhang et al., 2019; Chen et al., 2020). The peaks at 1,092 and 1,087 cm^{-1} were related to antisymmetric Si-O-Si vibration, and the peak at 800 cm^{-1} was related to Si-O stretching vibration (Chen et al., 2021). After adsorption, the peaks at 1,624 cm^{-1} moved to 1,581 cm^{-1} (PBC) and 1,578 cm^{-1} (TPBC), indicating that the biochar adsorbed TC. The peaks at 1,581 and 1,578 cm^{-1} are attributed to the stretching vibration of skeletal C = C (Zhang et al., 2019; Chen et al., 2020). The TPBC peak was slightly clearer than that of PBC, which could explain the higher TC adsorption capacity of TPBC.

XPS was used to investigate the adsorption mechanism. **Figures 9A,B** show that the PBC peak at 288.12 eV corresponds to carbon in the O–C = O group (Lei et al., 2014), whereas the XPS spectrum of TPBC did not show this peak, indicating that oxidative torrefaction could lead to the removal of the O–C = O group of PAS. Compared with **Figures 9C,D**, **Supplementary Figures 1A–D**, **2A–D**, the peaks of PBC and TPBC correspond to the C–C, C = C, C–O, C = O, C–N, and N-H groups shifted by varying degrees after adsorption, due to the increase in the corresponding functional group amount. Moreover, TPBC showed a peak at 288.03 eV after adsorption, which corresponds to carbon in the O–C = O group of TC. According to **Supplementary Figures 3A–D**, the peaks of PBC

and TPBC shifted by varying degrees after adsorption, which may correspond to changes in the Si-O group amount, confirming that ash content could participate in the adsorption process.

Comparison of Adsorption Capacities of Various Biochars for TC Removal

The capacity of TPBC to remove TC from aqueous solutions was compared with that of biochar produced from different types of biomass (**Table 6**). The comparison of Q_m implies that the adsorption capacity of the prepared biochar in this work is higher than that of the other six biochars (some of which were chemically modified) reported earlier for TC removal. The TPBC prepared by PAS pyrolysis combined with oxidative torrefaction in this work had a higher TC adsorption capacity than PBC. Therefore, oxidative torrefaction could be an effective approach to improve the adsorption capacity of PAS biochar for TC; and the use of PAS biochar could be recommended for the efficient treatment of wastewater containing TC, which could effectively remove TC and reduce the cost of biochar production.

CONCLUSION

The results of this study confirmed that oxidative torrefaction improved the TC adsorption capacity of PAS biochar. TPBC had higher specific surface area and lower ash content than PBC, which could be the result of devolatilization and thermal decomposition of PAS and of oxidation reactions during oxidative torrefaction. The adsorption kinetics showed a better correlation with the pseudo-second-order model. The isotherm and thermodynamics confirmed that the adsorption process is favorable and irreversible and that the dominant adsorption mode is physical. The FTIR and XPS results showed that oxidative torrefaction could lead to the removal of the O–C = O group of PAS and that the ash content could participate in the TC adsorption process. In addition, the capacity of TPBC to remove TC from aqueous solutions was higher than that of PBC and of several previously reported biochars produced from different types of biomass. In summary, the results of this study suggested that oxidative torrefaction could be an effective approach to improve the adsorption capacity of PAS biochar for TC; further, the use of biochar derived from oxidatively torrefied PAS pyrolysis could be recommended for the efficient treatment of wastewater containing TC. The results were satisfactory, which can provide not only a good idea for biomass utilization and torrefaction pretreatment for biomass upgrading, but also an effective adsorbent for the treatment of wastewater that contains tetracycline. However, oxidative torrefaction to improve the physicochemical properties of biochar requires more in-depth mechanism research, which could be the focus of future research in the field of biomass thermochemical conversion.

DATA AVAILABILITY STATEMENT

The original contributions presented in the study are included in the article/**Supplementary Material**, further inquiries can be directed to the corresponding author/s.

AUTHOR CONTRIBUTIONS

SJ and MT carried out all the experiments. SJ wrote the manuscript. JHu, CL, and TL offered technical guidance, supported in data analysis, and worked on the completed manuscript. XZ, ZW, J. Ha, and XQ assisted in designing the laboratory experiments, as well as in writing the manuscript. MT, JHu, and XZ assisted in checking and modifying the grammar of the manuscript. ZH and HL provided overall guidance, supervision, and scientific knowledge support for this research. All authors contributed to the article and approved the submitted version.

FUNDING

The authors gratefully acknowledge financial supports from the National Key R&D Program of China (2017YFC05055052), National Natural Science Foundation of China (51808216), Hunan Science and Technology Planning Project (2018RS3109), Science and Technology International Cooperation Project of Changsha City (kq1907082), Training Program for Excellent Young Innovators of Changsha (kq1905021 and kq1905020), Hunan Forestry Science and Technology Project (XLK201801, XLK201908, XLK201938, and XLK201901).

SUPPLEMENTARY MATERIAL

The Supplementary Material for this article can be found online at: https://www.frontiersin.org/articles/10.3389/fenrg.2021.673758/full#supplementary-material

Supplementary Figure 1 | The O1s XPS spectrum of PBC before **(A)** and after **(C)** adsorption and TPBC before **(B)** and after **(D)** adsorption.

Supplementary Figure 2 | The N1s XPS spectrum of PBC before **(A)** and after **(C)** adsorption and TPBC before **(B)** and after **(D)** adsorption.

Supplementary Figure 3 | The Si2p XPS spectrum of PBC before **(A)** and after **(C)** adsorption and TPBC before **(B)** and after **(D)** adsorption.

REFERENCES

Adebayo, M. A., Prola, L. D. T., Lima, E. C., Puchana-Rosero, M. J., Cataluña, R., Saucier, C., et al. (2014). Adsorption of procion blue MX-R dye from aqueous solutions by lignin chemically modified with aluminium and manganese. *J. Hazard. Mater.* 268, 43–50. doi: 10.1016/j.jhazmat.2014.01.005

Adesemuyi, M. F., Adebayo, M. A., Akinola, A. O., Olasehinde, E. F., Adewole, K. A., and Lajide, L. (2020). Preparation and characterisation of biochars from elephant grass and their utilisation for aqueous nitrate removal: effect of pyrolysis temperature. *J. Environ. Chem. Eng.* 8:104507. doi: 10.1016/j.jece.2020.104507

Ahmad, M. A., and Alrozi, R. (2011). Removal of malachite green dye from aqueous solution using rambutan peel-based activated carbon:

equilibrium, kinetic and thermodynamic studies. *Chem. Eng. J.* 171, 510–516.

Areco, M. M., Hanela, S., Duran, J., and dos Santos Afonso, M. (2012). Biosorption of Cu(II), Zn(II), Cd(II) and Pb(II) by dead biomasses of green alga *Ulva lactuca* and the development of a sustainable matrix for adsorption implementation. *J. Hazard. Mater.* 213-214, 123–132. doi: 10.1016/j.jhazmat.2012.01.073

Bach, Q. V., Trinh, T. N., Tran, K. Q., and Thi, N. B. D. (2017). Pyrolysis characteristics and kinetics of biomass torrefied in various atmospheres. *Energ. Convers. Manage.* 141, 72–78. doi: 10.1016/j.enconman.2016.04.097

Baghdadi, M., Ghaffari, E., and Aminzadeh, B. (2016). Removal of carbamazepine from municipal wastewater effluent using optimally synthesized magnetic activated carbon: adsorption and sedimentation kinetic studies. *J. Environ. Chem. Eng.* 4, 3309–3321. doi: 10.1016/j.jece.2016.06.034

Chabi, N., Baghdadi, M., Sani, A. H., Golzary, A., and Hosseinzadeh, M. (2020). Removal of tetracycline with aluminum boride carbide and boehmite particles decorated biochar derived from algae. *Bioresour. Technol.* 316:123950. doi: 10.1016/j.biortech.2020.123950

Chen, D., Li, Y., Deng, M., Wang, J., Chen, M., Yan, B., et al. (2016). Effect of torrefaction pretreatment and catalytic pyrolysis on the pyrolysis poly-generation of pine wood. *Bioresour. Technol.* 214, 615–622. doi: 10.1016/j.biortech.2016.04.058

Chen, D., Wang, X., Wang, X., Feng, K., Su, J., and Dong, J. (2020). The mechanism of cadmium sorption by sulphur-modified wheat straw biochar and its application cadmium-contaminated soil. *Sci. Total Environ.* 714:136550. doi: 10.1016/j.scitotenv.2020.136550

Chen, D., Zheng, Z., Fu, K., Zeng, Z., Wang, J., and Lu, M. (2015). Torrefaction of biomass stalk and its effect on the yield and quality of pyrolysis products. *Fuel* 159, 27–32. doi: 10.1016/j.fuel.2015.06.078

Chen, H., Chen, X., Qin, Y., Wei, J., and Liu, H. (2017). Effect of torrefaction on the properties of rice straw high temperature pyrolysis char: pore structure, aromaticity and gasification activity. *Bioresour. Technol.* 228, 241–249. doi: 10.1016/j.biortech.2016.12.074

Chen, Z., Pei, J., Wei, Z., Ruan, X., Hua, Y., Xu, W., et al. (2021). A novel maize biochar-based compound fertilizer for immobilizing cadmium and improving soil quality and maize growth. *Environ. Pollut.* 277:116455. doi: 10.1016/j.envpol.2021.116455

Divband Hafshejani, L., Hooshmand, A., Naseri, A. A., Mohammadi, A. S., Abbasi, F., and Bhatnagar, A. (2016). Removal of nitrate from aqueous solution by modified sugarcane bagasse biochar. *Ecol. Eng.* 95, 101–111. doi: 10.1016/j.ecoleng.2016.06.035

Doddapaneni, T., Konttinen, J., Hukka, T. I., and Moilanen, A. (2016). Influence of torrefaction pretreatment on the pyrolysis of Eucalyptus clone: a study on kinetics, reaction mechanism and heat flow. *Ind. Crop. Prod.* 92, 244–254. doi: 10.1016/j.indcrop.2016.08.013

dos Reis, G. S., Adebayo, M. A., Lima, E. C., Sampaio, C. H., and Prola, L. D. T. (2016). Activated carbon from sewage sludge for preconcentration of copper. *Anal. Lett.* 49, 541–555. doi: 10.1080/00032719.2015.1076833

Fleig, O. P., Raymundo, L. M., Trierweiler, L. F., and Trierweiler, J. O. (2021). Study of rice husk continuous torrefaction as a pretreatment for fast pyrolysis. *J. Anal. Appl. Pyrol.* 154:104994. doi: 10.1016/j.jaap.2020.104994

Gan, Y., Ong, H. C., Show, P. L., Ling, T., Chen, W., Yu, K., et al. (2018). Torrefaction of microalgal biochar as potential coal fuel and application as bio-adsorbent. *Energ. Convers. Manage.* 165, 152–162. doi: 10.1016/j.enconman.2018.03.046

Gao, Y., Li, Y., Zhang, L., Huang, H., Hu, J., Shah, S. M., et al. (2012). Adsorption and removal of tetracycline antibiotics from aqueous solution by graphene oxide. *J. Colloid Interf. Sci.* 368, 540–546. doi: 10.1016/j.jcis.2011.11.015

Gogoi, D., Bordoloi, N., Goswami, R., Narzari, R., Saikia, R., Sut, D., et al. (2017). Effect of torrefaction on yield and quality of pyrolytic products of arecanut husk: an agro-processing wastes. *Bioresour. Technol.* 242, 36–44. doi: 10.1016/j.biortech.2017.03.169

Gupta, S., Sireesha, S., Sreedhar, I., Patel, C. M., and Anitha, K. L. (2020). Latest trends in heavy metal removal from wastewater by biochar based sorbents. *J. Water Process Eng.* 38:101561. doi: 10.1016/j.jwpe.2020.101561

Huang, Z., Jiang, S., Guo, J., Wang, X., Tan, M., Xiong, R., et al. (2020). Oxidative torrefaction of *Phragmites australis*: gas-pressurized effects and correlation analysis based on color value. *Energ. Fuels* 34, 11073–11082. doi: 10.1021/acs.energyfuels.0c01974

Jang, H. M., and Kan, E. (2019). A novel hay-derived biochar for removal of tetracyclines in water. *Bioresour. Technol.* 274, 162–172. doi: 10.1016/j.biortech.2018.11.081

Khan, Z. H., Gao, M., Qiu, W., Islam, M. S., and Song, Z. (2020). Mechanisms for cadmium adsorption by magnetic biochar composites in an aqueous solution. *Chemosphere* 246:125701. doi: 10.1016/j.chemosphere.2019.125701

Lampropoulos, A., Kaklidis, N., Athanasiou, C., Montes-Morán, M. A., Arenillas, A., Menéndez, J. A., et al. (2020). Effect of Olive Kernel thermal treatment (torrefaction vs. slow pyrolysis) on the physicochemical characteristics and the CO_2 or H_2O gasification performance of as-prepared biochars. (in press). *Int. J. Hydrogen Energ.* doi: 10.1016/j.ijhydene.2020.11.230

Lei, P., Wang, F., Zhang, S., Ding, Y., Zhao, J., and Yang, M. (2014). Conjugation-grafted-TiO_2 nanohybrid for high photocatalytic efficiency under visible light. *ACS Appl. Mater. Inter.* 6, 2370–2376. doi: 10.1021/am4046537

Leng, L., Yuan, X., Huang, H., Wang, H., Wu, Z., Fu, L., et al. (2015). Characterization and application of bio-chars from liquefaction of microalgae, lignocellulosic biomass and sewage sludge. *Fuel Process. Technol.* 129, 8–14. doi: 10.1016/j.fuproc.2014.08.016

Liu, H., Xu, G., and Li, G. (2021). Preparation of porous biochar based on pharmaceutical sludge activated by NaOH and its application in the adsorption of tetracycline. *J. Colloid Interf. Sci.* 587, 271–278. doi: 10.1016/j.jcis.2020.12.014

Liu, J., Zhou, B., Zhang, H., Ma, J., Mu, B., and Zhang, W. (2019). A novel biochar modified by chitosan-Fe/S for tetracycline adsorption and studies on site energy distribution. *Bioresour. Technol.* 294:122152. doi: 10.1016/j.biortech.2019.122152

Lyu, H., Zhang, Q., and Shen, B. (2020). Application of biochar and its composites in catalysis. *Chemosphere* 240:124842. doi: 10.1016/j.chemosphere.2019.124842

Meng, J., Park, J., Tilotta, D., and Park, S. (2012). The effect of torrefaction on the chemistry of fast-pyrolysis bio-oil. *Bioresour. Technol.* 111, 439–446. doi: 10.1016/j.biortech.2012.01.159

Módenes, A. N., Bazarin, G., Borba, C. E., Locatelli, P. P. P., Borsato, F. P., Pagno, V., et al. (2021). Tetracycline adsorption by tilapia fish bone-based biochar: mass transfer assessment and fixed-bed data prediction by hybrid statistical-phenomenological modeling. *J. Clean. Prod.* 279:123775. doi: 10.1016/j.jclepro.2020.123775

Nguyen, V. T., Nguyen, T. B., Huang, C., Chen, C., Bui, X. T., and Dong, C. (2021). Alkaline modified biochar derived from spent coffee ground for removal of tetracycline from aqueous solutions. *J. Water Process Eng.* 40, 101908. doi: 10.1016/j.jwpe.2020.101908

Ntzoufra, P., Vakros, J., Frontistis, Z., Tsatsos, S., Kyriakou, G., Kennou, S., et al. (2021). Effect of sodium persulfate treatment on the physicochemical properties and catalytic activity of biochar prepared from spent malt rootlets. *J. Environ. Chem. Eng.* 9:105071. doi: 10.1016/j.jece.2021.105071

Peng, J., Bi, X., Sokhansanj, S., and Lim, C. J. (2013). Torrefaction and densification of different species of softwood residues. *Fuel* 111, 411–421. doi: 10.1016/j.fuel.2013.04.048

Ren, S., Lei, H., Wang, L., Bu, Q., Chen, S., and Wu, J. (2013). Thermal behaviour and kinetic study for woody biomass torrefaction and torrefied biomass pyrolysis by TGA. *Biosyst. Eng.* 116, 420–426. doi: 10.1016/j.biosystemseng.2013.10.003

Ren, S., Lei, H., Wang, L., Yadavalli, G., Liu, Y., and Julson, J. (2014). The integrated process of microwave torrefaction and pyrolysis of corn stover for biofuel production. *J. Anal. Appl. Pyrol.* 108, 248–253. doi: 10.1016/j.jaap.2014.04.008

Sanford, J. R., Larson, R. A., and Runge, T. (2019). Nitrate sorption to biochar following chemical oxidation. *Sci. Total Environ.* 669, 938–947. doi: 10.1016/j.scitotenv.2019.03.061

Song, Z., Ma, Y., and Li, C. (2019). The residual tetracycline in pharmaceutical wastewater was effectively removed by using MnO_2/graphene nanocomposite. *Sci. Total Environ.* 651, 580–590. doi: 10.1016/j.scitotenv.2018.09.240

Su, M., Azwar, E., Yang, Y., Sonne, C., Yek, P. N. Y., Liew, R. K., et al. (2020). Simultaneous removal of toxic ammonia and lettuce cultivation in aquaponic system using microwave pyrolysis biochar. *J. Hazard. Mater.* 396:122610. doi: 10.1016/j.jhazmat.2020.122610

Su, Y., Wen, Y., Yang, W., Zhang, X., Xia, M., Zhou, N., et al. (2021). The mechanism transformation of ramie biochar's cadmium adsorption by aging. *Bioresour. Technol.* 330:124947. doi: 10.1016/j.biortech.2021.124947

Taşkan, B., Casey, E., and Hasar, H. (2019). Simultaneous oxidation of ammonium and tetracycline in a membrane aerated biofilm reactor. *Sci. Total Environ.* 682, 553–560. doi: 10.1016/j.scitotenv.2019.05.111

Tumuluru, J. S. (2015). Comparison of chemical composition and energy property of torrefied switchgrass and corn stover. *Front. Energy Res.* 3:46. doi: 10.3389/fenrg.2015.00046

Uemura, Y., Sellappah, V., Trinh, T. H., Hassan, S., and Tanoue, K. (2017). Torrefaction of empty fruit bunches under biomass combustion gas atmosphere. *Bioresour. Technol.* 243, 107–117. doi: 10.1016/j.biortech.2017.06.057

Viglašová, E., Galamboš, M., Danková, Z., Krivosudský, L., Lengauer, C. L., Hood-Nowotny, R., et al. (2018). Production, characterization and adsorption studies of bamboo-based biochar/montmorillonite composite for nitrate removal. *Waste Manage.* 79, 385–394. doi: 10.1016/j.wasman.2018.08.005

Wang, S., Dai, G., Ru, B., Zhao, Y., Wang, X., Xiao, G., et al. (2017). Influence of torrefaction on the characteristics and pyrolysis behavior of cellulose. *Energy* 120, 864–871. doi: 10.1016/j.energy.2016.11.135

Wang, W., Gao, M., Cao, M., Dan, J., and Yang, H. (2021). Self-propagating synthesis of Zn-loaded biochar for tetracycline elimination. *Sci. Total Environ.* 759:143542. doi: 10.1016/j.scitotenv.2020.143542

Wang, Z., Guo, H., Shen, F., Yang, G., Zhang, Y., Zeng, Y., et al. (2015). Biochar produced from oak sawdust by Lanthanum (La)-involved pyrolysis for adsorption of ammonium (NH_4^+), nitrate (NO_3^-), and phosphate (PO_4^{3-}). *Chemosphere* 119, 646–653. doi: 10.1016/j.chemosphere.2014.07.084

Wannapeera, J., Fungtammasan, B., and Worasuwannarak, N. (2011). Effects of temperature and holding time during torrefaction on the pyrolysis behaviors of woody biomass. *J. Anal. Appl. Pyrol.* 92, 99–105. doi: 10.1016/j.jaap.2011.04.010

Xiang, W., Zhang, X., Chen, J., Zou, W., He, F., Hu, X., et al. (2020). Biochar technology in wastewater treatment: a critical review. *Chemosphere* 252:126539. doi: 10.1016/j.chemosphere.2020.126539

Xu, S., Li, J., Yin, Z., Liu, S., Bian, S., and Zhang, Y. (2020). A highly efficient strategy for enhancing the adsorptive and magnetic capabilities of biochar using Fenton oxidation. *Bioresour. Technol.* 315:123797. doi: 10.1016/j.biortech.2020.123797

Xu, Z., Zinchik, S., Kolapkar, S. S., Bar-Ziv, E., Hansen, T., Conn, D., et al. (2018). Properties of torrefied U.S. waste blends. *Front. Energy Res.* 6:65. doi: 10.3389/fenrg.2018.00065

Yu, H., Gu, L., Chen, L., Wen, H., Zhang, D., and Tao, H. (2020). Activation of grapefruit derived biochar by its peel extracts and its performance for tetracycline removal. *Bioresour. Technol.* 316:123971. doi: 10.1016/j.biortech.2020.123971

Yu, K., Show, P. L., Ong, H. C., Ling, T., Chi-Wei Lan, J., Chen, W., et al. (2017). Microalgae from wastewater treatment to biochar – Feedstock preparation and conversion technologies. *Energ. Convers. Manage.* 150, 1–13. doi: 10.1016/j.enconman.2017.07.060

Zhang, X., Li, Y., Wu, M., Pang, Y., Hao, Z., Hu, M., et al. (2021). Enhanced adsorption of tetracycline by an iron and manganese oxides loaded biochar: kinetics, mechanism and column adsorption. *Bioresour. Technol.* 320:124264. doi: 10.1016/j.biortech.2020.124264

Zhang, X., Mao, X., Pi, L., Wu, T., and Hu, Y. (2019). Adsorptive and capacitive properties of the activated carbons derived from pig manure residues. *J. Environ. Chem. Eng.* 7:103066. doi: 10.1016/j.jece.2019.103066

Zhang, Z., Gao, P., Cheng, J., Liu, G., Zhang, X., and Feng, Y. (2018). Enhancing anaerobic digestion and methane production of tetracycline wastewater in EGSB reactor with GAC/NZVI mediator. *Water Res.* 136, 54–63. doi: 10.1016/j.watres.2018.02.025

Zhu, X., Luo, Z., Diao, R., and Zhu, X. (2019a). Combining torrefaction pretreatment and co-pyrolysis to upgrade biochar derived from bio-oil distillation residue and walnut shell. *Energ. Convers. Manage.* 199:111970. doi: 10.1016/j.enconman.2019.111970

Zhu, X., Yuan, W., Lang, M., Zhen, G., Zhang, X., and Lu, X. (2019b). Novel methods of sewage sludge utilization for photocatalytic degradation of tetracycline-containing wastewater. *Fuel* 252, 148–156. doi: 10.1016/j.fuel.2019.04.093

Conflict of Interest: The authors declare that the research was conducted in the absence of any commercial or financial relationships that could be construed as a potential conflict of interest.